Phase Space for the Breakdown of the Quantum Hall Effect in Epitaxial Graphene

J. A. Alexander-Webber,[1] A. M. R. Baker,[1] T. J. B. M. Janssen,[2] A. Tzalenchuk,[2,3] S. Lara-Avila,[4] S. Kubatkin,[4] R. Yakimova,[5] B. A. Piot,[6] D. K. Maude,[6] and R. J. Nicholas[1,*]

[1]Department of Physics, University of Oxford, Clarendon Laboratory, Parks Road, Oxford OX1 3PU, United Kingdom
[2]National Physical Laboratory, Hampton Road, Teddington TW11 0LW, United Kingdom
[3]Department of Physics, Royal Holloway, University of London, Egham TW20 0EX, United Kingdom
[4]Department of Microtechnology and Nanoscience, Chalmers University of Technology, S-412 96 Göteborg, Sweden
[5]Department of Physics, Chemistry and Biology (IFM), Linköping University, S-581 83 Linköping, Sweden
[6]LNCMI-CNRS-UJF-INSA-UPS, 38042 Grenoble Cedex 9, France

(Received 17 April 2013; published 27 August 2013)

We report the phase space defined by the quantum Hall effect breakdown in polymer gated epitaxial graphene on SiC (SiC/G) as a function of temperature, current, carrier density, and magnetic fields up to 30 T. At 2 K, breakdown currents (I_c) almost 2 orders of magnitude greater than in GaAs devices are observed. The phase boundary of the dissipationless state ($\rho_{xx} = 0$) shows a $[1 - (T/T_c)^2]$ dependence and persists up to $T_c > 45$ K at 29 T. With magnetic field I_c was found to increase $\propto B^{3/2}$ and $T_c \propto B^2$. As the Fermi energy approaches the Dirac point, the $\nu = 2$ quantized Hall plateau appears continuously from fields as low as 1 T up to at least 19 T due to a strong magnetic field dependence of the carrier density.

DOI: 10.1103/PhysRevLett.111.096601 PACS numbers: 72.80.Vp, 72.10.Di, 73.43.Qt

The quantum Hall effect (QHE) observed in two-dimensional electron gases (2DEGs) is defined by a vanishing longitudinal resistivity $\rho_{xx} = 0$ and a quantized Hall resistance $\rho_{xy} = h/\nu e^2$ for $\nu =$ integer. Ever since its first observation [1] in silicon, the QHE has been used as a quantum electrical resistance standard which has been most extensively developed using GaAs devices [2]. In recent years, since the first isolation of graphene and the observation of the integer QHE [3,4], the attention of quantum Hall metrology labs has turned to graphene as a potentially more readily accessible resistance standard capable of operating at higher temperatures and measurement currents with lower magnetic fields. This is in part due to its large cyclotron energy gaps arising from the high electron velocity at the Dirac point. Recent experimental work [5] has also shown that it has high electron-phonon energy relaxation rates, an order of magnitude faster than in GaAs heterostructures, which play an important role in determining the high current breakdown of the QHE. In particular, polymer gated epitaxial graphene on SiC has been shown to be an exceptional candidate for metrology [6,7], and the universality of quantization between it and GaAs has been shown to be accurate within a relative uncertainty of 8.6×10^{-11} [8].

If epitaxial graphene is to be used as a quantum resistance standard, it is important to understand the experimental limits which confine the phase space where the accurate, dissipationless QHE can be observed. Such a phase space is determined by temperature T, carrier density n, magnetic field B, and current I. The breakdown of the QHE is defined as the point where deviations from quantization $\Delta\rho_{xy}$ can be observed, and this is strongly correlated with the point where $\rho_{xx} \neq 0$. A linear relationship of $\Delta\rho_{xy} \propto s\rho_{xx}$ is typically observed in GaAs [9] and recently in graphene [10,11], with typical values of $s \sim 0.1$ [2]; therefore, measurement of the $I - V_{xx}$ characteristics in the quantum Hall regime also determines the maximum current consistent with maintaining a quantized ρ_{xy}. At high currents, a sudden onset of longitudinal resistance is observed [2,7,12] above a critical current I_c. In GaAs and InSb, the temperature dependence [13–15] of I_c has been shown to be of the form

$$I_c(T) = I_c(0)\left(1 - \frac{T^2}{T_c^2}\right), \tag{1}$$

where T_c is the temperature at which $I_c = 0$, leading Rigal *et al.* [15] to draw parallels with a phase diagram as predicted by the Gorter-Casimir two-fluid model for superconductors. We will show that this also describes the temperature dependence of I_c very well in epitaxial graphene and will examine the magnetic field dependence of T_c, providing further support for the description of the dissipationless quantum Hall regime in terms of a phase diagram. Although the quantum Hall effect has already been reported in graphene at room temperature using magnetic fields of 45 T [16], the plateaus did not show exact quantization, as the resistivity was still finite ($\sim$10 Ω) and the system had not entered the dissipationless state. In this work, we address the formation of the zero-resistance state which corresponds to the full quantum Hall condition.

Two devices were studied, prepared from epitaxially grown graphene on the Si-terminated face of SiC. Each device was lithographed using an e-beam and oxygen plasma etching into an eight leg Hall bar geometry ($W/L = 4.5$) with widths of $W = 5$ μm and $W = 35$ μm for sample 1 and sample 2, respectively. Samples were

 © 2013 American Physical Society

electrically connected with large area Ti-Au contacting. A polymer gating technique using room temperature UV illumination was used to vary the electron density from $1\text{–}16 \times 10^{11}$ cm^{-2} as described in Ref. [17]. DC magnetotransport and $I - V$ data were taken using magnetic fields from a 21 T superconducting solenoid and a 30 T 20 MW resistive-coil magnet at the LNCMI Grenoble.

Figure 1(b) shows ρ_{xx} and ρ_{xy} for sample 1 with $n_{B=0} = 6.5 \times 10^{11}$ cm^{-2}. We observe Shubnikov–de Haas oscillations in filling factors up to $\nu = 8$, and a $\nu = 2$ quantum Hall plateau beginning at $B = 8$ T with $\rho_{xx} = 0$ from $B = 10$ T. This $\nu = 2$ state is over 20 T wide and observable all the way up to the maximum magnetic field of 30 T. A series of $I - V_{xx}$ traces was taken every Tesla along the plateau to investigate the breakdown, with typical examples in Fig. 1(a) at $T = 2$ K. At 23 T, we find $V_{xx} = 0$ until $I = I_c = 215$ μA, where we define the critical breakdown current at $V_{xx}(I_c) = 10$ μV, just above the noise level of our measurements [Fig. 1(a)], corresponding to a resistivity of $\rho_{xx} \approx 0.01$ Ω consistent

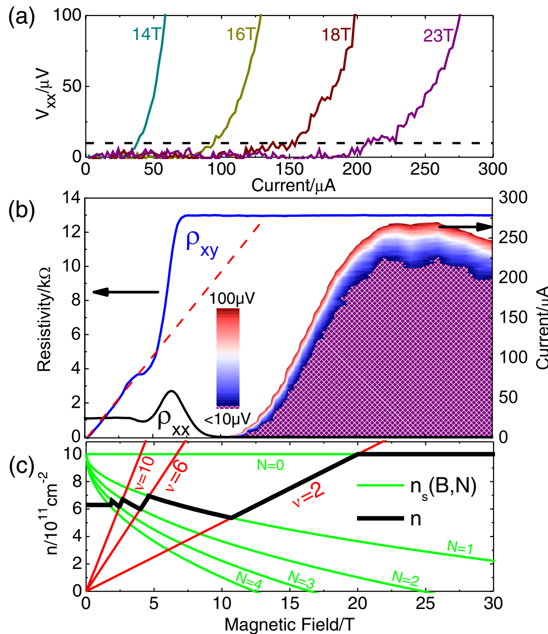

FIG. 1 (color online). (a) $I - V_{xx}$ characteristics of sample 1 at 2.0 K, with a breakdown condition of $V_{xx} = 10$ μV, giving a maximum critical current density $j_c = 43$ A/m at 23 T. (b) Combined magnetotransport [ρ_{xy} and ρ_{xx}] data and $I - V_{xx} - B$ contour plot; the hashed region represents $V_{xx} <$ 10 μV, the dissipationless quantum Hall regime. Extrapolating the low field Hall coefficient to $\rho_{xy} = h/2e^2$ (dashed red line) gives the expected field for the peak breakdown of $\nu = 2$ without a field dependent n. (c) Magnetic field dependence of the carrier density (thick black line), following lines of constant filling factor (thin red lines) while E_F lies between Landau levels and then the charge transferred from surface donors in SiC, $n(B, N)$ (thin green curves), while the Landau levels fill, from the model in Ref. [7].

with a quantization accuracy of better than 1 in 10^7. Such a high breakdown current for a device just 5 μm wide, giving a critical current density of $j_c = 43$ A/m, is truly exceptional in comparison to even the most well optimized GaAs devices, where $j_c^{\mathrm{GaAs}} \sim 1\text{–}2$ A/m [2,12]. The full set of $I - V_{xx}$ traces is plotted in Fig. 1(b) as a contour plot. The hashed region is therefore the phase space where the dissipationless QHE is observed. The critical current I_c increases along the plateau with a peak around 23 T. Unlike traditional semiconductor quantum Hall systems which show a very sharp peak in I_c centered at integer filling factor [13], the peak breakdown current occurs at fields much greater than $\nu = 2$ calculated from the zero-field carrier density and changes very little in magnitude over a wide range of fields. This is due to the strong magnetic field dependence of the carrier density in epitaxial graphene grown on Si-terminated SiC [18]. Carriers are transferred to the graphene from the surface donor states of the SiC which are assumed to have a constant density of states. The charge transfer $n_s(B, N)$ is proportional to the difference between the work function of the graphene and the SiC. This causes the unbroadened Landau levels to be completely filled over a wide range of magnetic fields [7], particularly when the Fermi energy E_F is between the $N = 0$ and $N = 1$ Landau levels, as in the region above 11 T in Fig. 1(c). Assuming that the peak I_c occurs at $\nu = 2$ suggests that the carrier density has increased to $n = 1.1 \times 10^{12}$ cm^{-2} by 23 T and is still increasing. As a result, the breakdown current is relatively independent of magnetic field, which adds to the convenience of epitaxial graphene as an electrical resistance standard.

At the lowest carrier density studied using sample 2 ($n_{B=0} \sim 1 \times 10^{11}$ cm^{-2}), the $\nu = 2$ state [Fig. 2(a)] begins at $B = 1$ T and persists up to the maximum field studied for this sample of 19 T. The breakdown current shown in Fig. 2(a) is negligible at low fields ($B < 3$ T) but rapidly increases reaching a peak at $B = 7$ T, suggesting a carrier density of $n_{B=7\ \mathrm{T}} = 3.5 \times 10^{11}$ cm^{-2}. At 7 T, $I_c =$ 140 μA, giving $j_c = 4$ A/m for this 35 μm wide device. Importantly, from an applications perspective, $I_c \sim$ 100 μA by 5 T, a magnetic field which is readily accessible with simple bench top magnets and where a current of 100 μA has been shown to be sufficient to obtain an accuracy of a few parts in 10^{11} when comparing $h/2e^2$ in graphene and GaAs [8,11]. Applying the charge transfer model [18], the magnetic field for peak breakdown is accurately predicted [Fig. 2(b)], but above this no further increase in carrier density is expected due to the finite density of donor states. The data suggest that the carrier density is still increasing, as the breakdown current has only decreased by a factor of 1.8 by 19 T, probably due to the influence of level broadening which is not included in the original model [18]. In typical semiconductor 2DEGs [2,13], breakdown currents show a triangular behavior with a plateau width [defined by $I_c(\nu)/I_c \geq 0$]

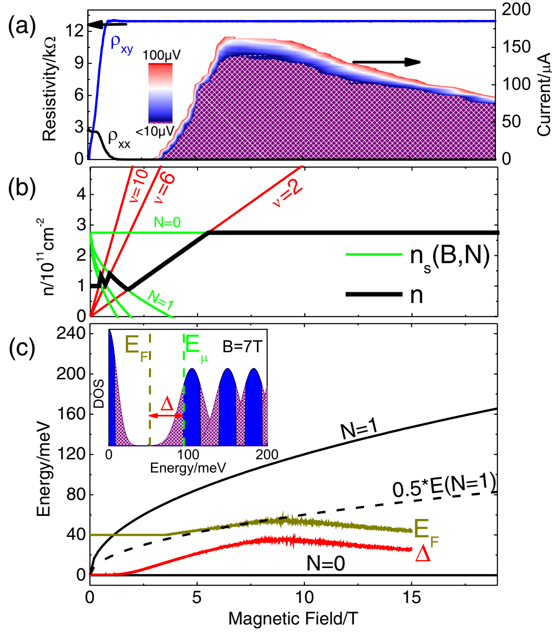

FIG. 2 (color online). (a) Magnetotransport [ρ_{xy} and ρ_{xx}] and corresponding $I - V_{xx} - B$ contour plot for the 35 μm wide device at $T = 1.5$ K. (b) Theoretical prediction of magnetic field dependent carrier density (thick black line) as descibed for Fig. 1 [18]. (c) Δ as a function of magnetic field and the resulting E_F. Also shown are the $N = 0$ and 1 Landau levels (black curves) and the midpoint where $E_F = 1/2E(N = 1)$ corresponding to $\nu = 2$.

of $\Delta\nu/\nu \sim \pm 0.2$. Assuming a level degeneracy (η) of four for the $\nu = 2$ plateau due to the valley and spin degeneracies in graphene, this should correspond to a total plateau width of $\Delta\nu = \pm 0.8$, and I_c should halve by 9 T ($\nu = 1.6$). This is consistent with results reported for exfoliated graphene [19]. By contrast, the slow decrease in I_c seen in Fig. 2(a) suggests that the occupancy remains $\nu \geq 1.6$ up to 19 T, where the carrier density has increased to $n \geq 7 \times 10^{11}$ cm^{-2}.

An Arrhenius analysis of the activated conductivity at higher temperatures (50–100 K), above the variable range hopping regime [20,21], was used to estimate the magnetic field dependence of the Fermi energy E_F by measuring the activation gap Δ as a function of magnetic field. We assume that this measures the separation of E_F from the conducting states E_μ of the nearest Landau level ($N = 1$ for $B < 7$ T, $N = 0$ for $B > 7$ T), where $\Delta = |E_\mu - E_F|$. Figure 2(c) shows Δ and the value of E_F which has been deduced by assuming that it is midway between the two Landau levels at 7 T where $\nu = 2$. At low fields, E_F corresponds to the approximately constant value of 40 meV deduced from the low field carrier density. Above 2.5 T, the carrier density begins to increase due to charge transfer from the substrate which keeps the Fermi energy in the gap between $N = 1$ and $N = 0$, and the system enters the dissipationless quantum Hall state. Above 7 T, E_F falls slightly but appears pinned close to a constant energy of $E_F \sim 40$ meV, suggesting that there may be a specific surface impurity level close to this value. This suggests that the $\nu = 2$ plateau could extend up to higher fields still until the extended states of the symmetry broken $N = 0$ state pass through the pinned Fermi level.

High temperature ($T > 4$ K) operation is also highly desirable for an accessible resistance standard. We have studied the temperature dependence of the dissipationless phase for several carrier densities for the peak I_c at $\nu = 2$, and for the highest carrier density of $n = 1.6 \times 10^{12}$ cm^{-2} at 29 T, as the maximum I_c was just beyond our maximum field. Figure 3(a) shows that Eq. (1) also describes the temperature dependence of I_c for the dissipationless state very well in epitaxial graphene. In addition to the analogy with superconductors [15], this form has also been suggested by Tanaka *et al.* [14] based on a model which predicts this behavior from a temperature-dependent mobility edge caused by the temperature dependence of the tunneling probabilites from localized to extended states at the center of the Landau levels. Experimentally, only limited evidence exists for the dependence of T_c on magnetic field with values for GaAs [14,15] of $T_c/B \approx 1$ K/T for B values of 4.8–7.7 T at $\nu = 4$ and $T_c \propto 1/\nu$, while for InSb $T_c = 8$ K at 6.1 T [13]. It is therefore surprising that for graphene, we see a strong superlinear scaling, as shown in Fig. 3(b) with a best fit of approximately $T_c \propto B^2$, which extrapolates to $T_c = 111$ K at 45 T. The rate of increase of the cyclotron energy gap between the $N = 1$ and $N = 0$ Landau levels is sublinear, given by $E_N = \mathrm{sgn}(N) \times c^*\sqrt{2e\hbar B|N|}$, where c^* is the electron velocity, suggesting a weaker overall field dependence. One significant difference in epitaxial graphene is the magnitude of the disorder,

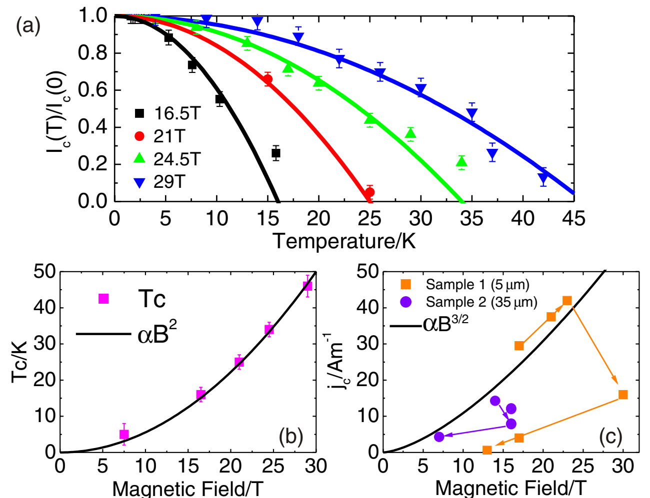

FIG. 3 (color online). (a) Normalized temperature dependence of breakdown current at several magnetic fields, fitted with Eq. (1). (b) The magnetic field dependence of T_c, with a best fit of $0.055B^2$. (c) The magnetic field dependence of j_c for the two Hall bars with the sequence of illumination shown by arrows.

TABLE I. Material comparison for QHE breakdown at $\nu = 2$.

Material	$\hbar\omega_c$ (meV)	τ_e (ps)	j_c (A m^{-1}) Theory [22]	j_c (A m^{-1}) Experiment	Width (μm)
GaAs (7 T)	12	100 [31]	2.9	1.4	35 [14]
InSb (7 T)	40	500 [13]	2.6	0.3	600 [13]
Graphene (7 T)	105	80 [24]	7.3	**4.3**	35
(14 T)	150	30 [24]	23	**15**	35
(17 T)	165	16 [24]	36	**30**	5
(23 T)	200	6 [24]	71	**43**	5

which means that the activation energy $\Delta = |E_\mu - E_F|$ at $\nu = 2$ has a large offset due to level broadening and is known to increase more rapidly than the cyclotron energy [20] due possibly to smaller broadening for the $N = 0$ Landau level which is topologically protected [3].

By contrast, I_c has been extensively studied and is well known experimentally to scale as $B^{3/2}$ [2,12,14] as predicted by several of the models for breakdown [22] which include factors for the cyclotron energy and the inverse magnetic length. Figure 3(c) shows the values for $j_c = I_c/W$ at $\nu = 2$ for both samples after each UV illumination. The highest values observed are after some UV illumination and are consistent with the $B^{3/2}$ dependence, although there can be significant falls after extended illumination. This is probably because the spatial inhomogeneities have become greater, which is likely to reduce j_c. Interestingly, despite the spread of j_c values, the same samples produced the very clear systematic dependence of T_c shown in Fig. 3, supporting the phase diagrammatic picture of the dissipationless state. It should be noted that the values are somewhat higher for the 5 μm Hall bars and there is some evidence that quantum Hall breakdown current densities are slightly larger for smaller Hall bar widths [2,23].

The most widely accepted theory for the QHE breakdown is the bootstrap electron heating model proposed by Komiyama and Kawaguchi [22] in which the quantum Hall state becomes thermally unstable above a critical Hall electric field where the rate of change of the electron-phonon energy loss rate becomes less than the rate of increase of input power. This predicts a critical breakdown electric field of

$$E_c = j_c \rho_{xy} = \sqrt{\frac{4B\hbar\omega_c}{\eta e \tau_e}}, \qquad (2)$$

where τ_e is a characteristic electron-phonon energy relaxation time and $\eta = 4$. Recently, much experimental [24–27] and theoretical [28] interest has focused on the way hot electrons lose energy to the lattice in graphene. We use the values of τ_e, observed at T_c as measured previously from the damping of Shubnikov–de Haas oscillations [13,24,29,30] to calculate the predicted j_c for $\nu = 2$ and compare these to conventional semiconductor 2DEGs in Table I. The theoretical and experimental values of j_c in graphene are considerably larger, as compared, for example, to InSb, which has the lowest mass of the III–V semiconductors $m^* = 0.02 m_e$ [32]. At 7 T, the cyclotron energy gap is 105 meV for graphene, compared to 40 meV in InSb; however, we find an order of magnitude increase in current density for graphene over InSb. This is mainly a result of the factor 6 difference in τ_e between the two systems. The increase of T_c with field causes τ_e to decrease and the dependence of j_c on magnetic field to be superlinear.

In summary, we have investigated the phase space in which the dissipationless quantum Hall state exists for epitaxial graphene. The data support the idea that this system can be described in terms of a phase diagram for the dissipationless state where the temperature dependence of the critical current follows a behavior $\propto [1 - (T/T_c)^2]$ as seen in GaAs and InSb quantum Hall systems, providing strong evidence that this is a general feature of the quantum Hall state for a wide range of magnetic fields, temperatures, and different materials. We demonstrate that both the critical temperature and current are strongly magnetic field dependent and that at high fields, critical current densities can be more than a factor 30 larger than previously observed in other systems. In epitaxial graphene, charge transfer from the carbon layer between the graphene and the SiC substrate also leads to a strongly magnetic field dependent carrier density and an exceptionally wide $\nu = 2$ plateau due to charge transfer from surface impurities followed by pinning to a constant energy associated with a surface impurity level.

This work was supported by EuroMagNET II, EU Contract No. 228043, EU Project ConceptGraphene, NPL Strategic Research Programme, and by the U.K. EPSRC.

*r.nicholas@physics.ox.ac.uk

[1] K. von Klitzing, G. Dorda, and M. Pepper, Phys. Rev. Lett. **45**, 494 (1980).

[2] B. Jeckelmann and B. Jeanneret, Rep. Prog. Phys. **64**, 1603 (2001).

[3] K. S. Novoselov, A. K. Geim, S. V. Morozov, D. Jiang, M. I. Katsnelson, I. V. Grigorieva, S. V. Dubonos, and A. A. Firsov, Nature (London) **438**, 197 (2005).

[4] Y. Zhang, Y. W. Tan, H. L. Stormer, and P. Kim, Nature (London) **438**, 201 (2005).
[5] A. M. R. Baker, J. A. Alexander-Webber, T. Altebaeumer, and R. J. Nicholas, Phys. Rev. B **85**, 115403 (2012).
[6] A. Tzalenchuk, S. Lara-Avila, A. Kalaboukhov, S. Paolillo, M. Syväjärvi, R. Yakimova, O. Kazakova, T. J. B. M. Janssen, V. Fal'ko, and S. Kubatkin, Nat. Nanotechnol. **5**, 186 (2010).
[7] T. J. B. M. Janssen, A. Tzalenchuk, R. Yakimova, S. Kubatkin, S. Lara-Avila, S. Kopylov, and V. I. Fal'ko, Phys. Rev. B **83**, 233402 (2011).
[8] T. J. B. M. Janssen, N. E. Fletcher, J. M. Goebel, R. Williams, A. Tzalenchuk, R. Yakimova, S. Kubatkin, S. Lara-Avila, and V. I. Fal'ko, New J. Phys. **13**, 093026 (2011).
[9] M. E. Cage, B. F. Field, R. F. Dziuba, S. M. Girvin, A. C. Gossard, and D. C. Tsui, Phys. Rev. B **30**, 2286 (1984).
[10] J. Guignard, D. Leprat, D. C. Glattli, F. Schopfer, and W. Poirier, Phys. Rev. B **85**, 165420 (2012).
[11] T. J. B. M. Janssen, J. M. Williams, N. E. Fletcher, R. Goebel, A. Tzalenchuk, R. Yakimova, S. Lara-Avila, S. Kubatkin, and V. I. Fal'ko, Metrologia **49**, 294 (2012).
[12] W. Poirer and F. Schopfer, Eur. Phys. J. Special Topics **172**, 207 (2009).
[13] J. A. Alexander-Webber, A. M. R. Baker, P. D. Buckle, T. Ashley, and R. J. Nicholas, Phys. Rev. B **86**, 045404 (2012).
[14] H. Tanaka, H. Kawashima, H. Iizuka, H. Fukuda, and S. Kawaji, J. Phys. Soc. Jpn. **75**, 014701 (2006).
[15] L. B. Rigal, D. K. Maude, M. Potemski, J. C. Portal, L. Eaves, J. R. Wasilewski, G. Hill, and M. A. Pate, Phys. Rev. Lett. **82**, 1249 (1999).
[16] K. S. Novoselov, Z. Jiang, Y. Zhang, S. V. Morozov, H. L. Stormer, U. Zeitler, J. C. Maan, G. S. Boebinger, P. Kim, and A. K. Geim, Science **315**, 1379 (2007).
[17] S. Lara-Avila, K. Moth-Poulsen, R. Yakimova, T. Bjørnholm, V. Fal'ko, A. Tzalenchuk, and S. Kubatkin, Adv. Mater. **23**, 878 (2011).
[18] S. Kopylov, A. Tzalenchuk, S. Kubatkin, and V. I. Fal'ko, Appl. Phys. Lett. **97**, 112109 (2010).
[19] M. Amado, E. Diez, F. Rossella, V. Bellani, D. Lopez-Romero, and D. K. Maude, J. Phys. Condens. Matter **24**, 305302 (2012).
[20] A. J. M. Giesbers, U. Zeitler, M. I. Katsnelson, L. A. Ponomarenko, T. M. Mohiuddin, and J. C. Maan, Phys. Rev. Lett. **99**, 206803 (2007).
[21] K. Bennaceur, P. Jacques, F. Portier, P. Roche, and D. C. Glattli, Phys. Rev. B **86**, 085433 (2012).
[22] S. Komiyama and Y. Kawaguchi, Phys. Rev. B **61**, 2014 (2000).
[23] Y. M. Meziani, C. Chaubet, S. Bonifacie, A. Raymond, W. Poirier, and F. Piquemal, J. Appl. Phys. **96**, 404 (2004).
[24] A. M. R. Baker, J. A. Alexander-Webber, T. Altebaeumer, S. D. McMullan, T. J. B. M. Janssen, A. Tzalenchuk, S. Lara-Avila, S. Kubatkin, R. Yakimova, C.-T. Lin *et al.*, Phys. Rev. B **87**, 045414 (2013).
[25] A. Betz, F. Vialla, D. Brunel, C. Voisin, M. Picher, A. Cavanna, A. Madouri, G. Feve, J.-M. Berroir, B. Placais *et al.*, Phys. Rev. Lett. **109**, 056805 (2012).
[26] Z. Tan, C. Tan, L. Ma, G. T. Liu, L. Lu, and C. L. Yang, Phys. Rev. B **84**, 115429 (2011).
[27] A. C. Betz, S. H. Jhang, E. Pallecchi, R. Ferreira, G. Fève, J.-M. Berroir, and B. Plaçais, Nat. Phys. **9**, 109 (2013).
[28] S. S. Kubakaddi, Phys. Rev. B **79**, 075417 (2009).
[29] D. R. Leadley, R. J. Nicholas, J. J. Harris, and C. T. Foxon, Solid State Electron **32**, 1473 (1989).
[30] See Supplemental Material at http://link.aps.org/supplemental/10.1103/PhysRevLett.111.096601 for discussion of the measurement of τ_e.
[31] D. R. Leadley, R. J. Nicholas, J. J. Harris, and C. T. Foxon, Semicond. Sci. Technol. **4**, 879 (1989).
[32] J. M. S. Orr, K. C. Chuang, R. J. Nicholas, L. Buckle, M. T. Emeny, and P. D. Buckle, Phys. Rev. B **79**, 235302 (2009).